



OPEN ACCESS

EDITED BY

Xuelong Li,
Shandong University of Science and
Technology, China

REVIEWED BY

Chaoyu Chang,
Institute of Disaster Prevention, China
Anquan Xu,
Tianjin University, China

*CORRESPONDENCE

Zhongfa Guo,
✉ xjr2458023298@sina.com
Dewen Liu,
✉ civil_liudewen@sina.com
Weiwei Sun,
✉ 861981546@qq.com

RECEIVED 06 July 2023

ACCEPTED 09 August 2023

PUBLISHED 14 September 2023

CITATION

Xu J, Gao H, Guo Z, Zhao J, Yang Z,
Zhao G, Guo Z, Liu D and Sun W (2023),
Key technologies research on of soil-
structure interaction base story isolated
structure response in 3D seismic zone.
Front. Earth Sci. 11:1254042.
doi: 10.3389/feart.2023.1254042

COPYRIGHT

© 2023 Xu, Gao, Guo, Zhao, Yang, Zhao,
Guo, Liu and Sun. This is an open-access
article distributed under the terms of the
[Creative Commons Attribution License
\(CC BY\)](https://creativecommons.org/licenses/by/4.0/). The use, distribution or
reproduction in other forums is
permitted, provided the original author(s)
and the copyright owner(s) are credited
and that the original publication in this
journal is cited, in accordance with
accepted academic practice. No use,
distribution or reproduction is permitted
which does not comply with these terms.

Key technologies research on of soil-structure interaction base story isolated structure response in 3D seismic zone

Jingran Xu¹, Haolun Gao¹, Zihan Guo¹, Jie Zhao¹, Zhuoxin Yang¹,
Guangxing Zhao¹, Zhongfa Guo^{2*}, Dewen Liu^{1*} and Weiwei Sun^{1*}

¹Southwest Forestry University, Kunming, Yunnan Province, China, ²Rattana Bundit University, Bangkok, Thailand

The development of karst in Karst area leads to poor stability of stratum. If earthquake occurs, the area will produce destructive disaster. In order to improve the stability capacity of the grassroots in the region, this study investigates the seismic response of inter-story isolation structures considering soil-structure interaction (SSI) in three-dimensional earthquakes. A model of the inter-story isolation structure incorporating SSI was developed, and one-dimensional, two-dimensional, and three-dimensional ground motions were applied to compare the seismic response under different input conditions. A three-dimensional isolation system was introduced and compared with traditional horizontal isolation structures to address excessive tensile and compressive stresses on the isolation structure during three-dimensional ground motion. The results demonstrate that the seismic response to three-dimensional earthquakes surpasses one-dimensional and two-dimensional inputs. Furthermore, adding a three-dimensional isolation structure effectively isolates vertical ground motion and reduces structural seismic response. Moreover, it minimizes soil stresses on the foundation compared to traditional horizontal isolation structure, enhancing foundation stability. This study will provide theoretical value and practical guidance for the research on key technology of SSI base story isolation structure response in Karst Plateau 3D Seismic zone.

KEYWORDS

karst, three-dimensional seismic zone, soil structure interaction, vibration isolation structure, key technology

1 Introduction

Inter-story seismic isolation is a novel technology developed based on base isolation principles, which has shown progress (Peng and Dong, 2023; Ehsan and Toopchi-Nezhad, 2023; Wan et al., 2023; Fan et al., 2023; Liang et al., 2023; Davide and Kalfas Konstantinos, 2023; Zhang et al., 2021; Zhang et al., 2021; Basili and Angelis, 2022; Hur and Park, 2022; Li et al., 2022). The Tokyo Shiodome Sumitomo Mansion (Toshiyuki et al., 2008), utilizing an inter-story isolated structure, effectively mitigates seismic response by incorporating an isolation story within the middle of the building. Bernardi et al. (2023) introduced a multi-objective optimization method to consider the overall structural response. They investigated the application of Inter-Story Isolation (IIS) as a Tuned Mass Damper (TMD) for structural tuning and derived new design equations accordingly. Three structural cases

underwent time history analysis to evaluate the optimization effects of this approach. The findings demonstrated that IIS improved the lower structural performance to some extent while also restraining isolation displacement and upper structural acceleration during seismic events. Zhou et al. (2016) developed a simple two-degree-of-freedom model using a streamlined reduction method based on modal synthesis. This model effectively captures the response characteristics of the entire system and facilitates the development of an analysis method for optimizing the parameters of the inter-story isolation system. Numerical examples were employed to explore the impact of different floor placements of the best inter-story isolation system within the same building, confirming the capability of isolation devices to reduce the structure's seismic response.

Zhang et al. (2017) proposed using Real-Time Hybrid Simulation (RTHS) to study the performance of buildings equipped with inter-story isolation. The shaking table serves as a means to establish essential boundary conditions. This study conducted experimental tests and numerical simulations on the substructures above and below the isolation story. Specifically, a 14-story building with inter-story isolation was subjected to a shaking table experiment controlled using an acceleration tracking method. The results demonstrated the accuracy and reliability of RTHS in investigating buildings with inter-story isolation. Tasaka et al. (2008) presented examples of base and inter-story isolation systems designed and refurbished by NIKKEN, a Japanese architectural and engineering company. The renovation project focused on retrofitting the base-isolation system while retaining the original structure, thereby enhancing its seismic performance. Furthermore, inter-story isolation systems can be applied to mid to high-rise buildings. Faiella et al. (2022) examined a three-story brick and stone building with an irregular structural configuration. The study addressed identifying dynamic parameters associated with the upper structure on the isolation story and required a comprehensive analysis of the lumped mass model to minimize the earthquake response. To establish standardized guidelines for the overall seismic response of buildings equipped with inter-story isolation structures, a detailed analysis of the Inter-Story Isolation (IIS) structure was conducted using a three-dimensional finite element model. The research findings were the basis for drawing conclusive opinions and proposing general design guidelines. Jin et al. (2012), Song et al. (2023) conducted experimental investigations into the seismic response and effectiveness of the mid-story isolation system in a four-story steel frame model. Various placements of the isolation story were considered, including the bottom of the first floor, the top of the first floor, the top of the second floor, and the top of the third floor.

The research outcomes revealed that the mid-story isolation system generally reduces seismic response, although it may amplify the acceleration of the lower structure of the isolation story. Additionally, applying mid-story isolated structures in reinforcing existing structures (Toshiyuki et al., 2008; Basili and Angelis, 2022; Zhang et al., 2022; Davide and Kalfas Konstantinos, 2023; Ehsan and Toopchi-Nezhad, 2023; Liu et al., 2023a; Liu et al., 2023a; Liu et al., 2023b; Li et al., 2023) effectively lowers the seismic response. Furthermore, machine learning methods have been employed to predict disaster occurrences in different environments (Huang et al., 2020a; Gao et al., 2023; Zhang et al., 2023). The structure development process (Liao et al., 2001; Li et al., 2014; Huang et al., 2020b; Zhang et al., 2021; Huang et al., 2022; Li et al.,

2022; Liu et al., 2022) has undergone significant advancements. Ryan and Earl, (2010) conducted a systematic study on the relationship between the effectiveness of inter-story isolation systems and their locations. They extensively explored the selection of isolation system parameters to achieve optimal performance. The research revealed that the single-story isolation system responds distinctively to the overall structure, effectively mitigating forces from above the isolation system but showing lesser effectiveness in reducing the strength of the structure below. To address practical challenges and ensure commercial feasibility, the study aimed to alleviate the forces acting on the structure below the isolation system by designing an inter-story isolation system suitable for light loads. Bolvardi et al. (2018) investigated the utilization of inter-story isolation systems in platform-type figure-rise Cross-Laminated Timber (CLT) buildings. Modifications were made to the displacement-based Generalized Direct Design (DDD) program to identify key design parameters of the inter-story isolation system required to achieve pre-selected displacement targets for the building. The proposed design program was applied to a 12-story CLT building design example using seismic hazard parameters specific to Los Angeles, California. The building's performance was numerically validated through nonlinear time history simulation.

Basili and Angelis, (2022), Liu and Li, (2023) conducted shaking table experiments on frame structures using a multi-degree-of-freedom setup. Three different structural configurations were tested, including a four-story, three-story intermediate, and three-story structure equipped with an unconventional Tuned Mass Damper (TMD). The experiments subjected the structures to input motion conditions such as white noise, sine sweep, and natural earthquake excitations. The study observed different dynamic behaviors for each test configuration, and the employed isolators demonstrated significant dissipation capacity across a wide range of excitation amplitudes. Moreover, the study highlighted the controlling effect of unconventional TMD in enhancing structural vibration reduction. The studies above have primarily focused on the structural response to horizontal ground motion. However, there is a research gap regarding the investigation of the seismic response of inter-story seismic isolation systems considering the Soil-Structure Interaction (SSI) effect under three-dimensional ground motion, which still needs to be explored by scholars. To address this gap, we establish a model for inter-story seismic isolation that accounts for the SSI effect. One-dimensional, two-dimensional, and three-dimensional ground motions are separately applied as input parameters. By comparing the seismic responses of inter-story seismic isolation under different dimensional seismic wave inputs, we aim to address the research questions and provide solutions to the identified challenges.

2 Methods and materials

2.1 Methods

2.1.1 Centrally concentrated viscoelastic artificial boundary with fixed base

In the study considering Soil-Structure Interaction (SSI) effects, a continuous distribution of viscoelastic artificial boundaries is employed. When discretizing the problem using finite element

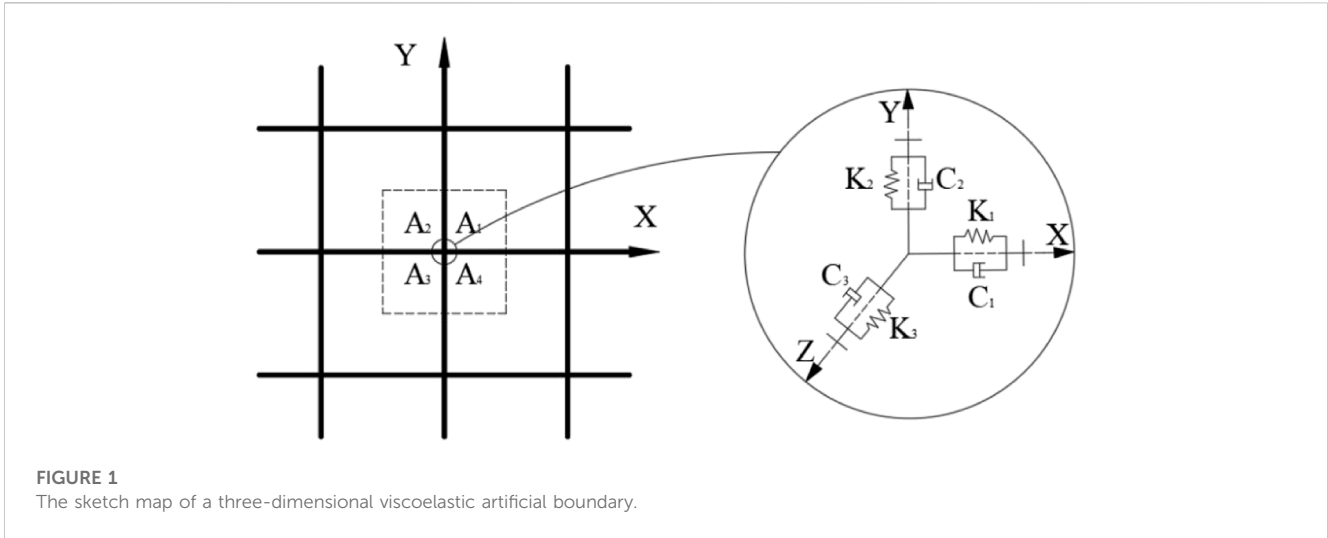


FIGURE 1
The sketch map of a three-dimensional viscoelastic artificial boundary.

TABLE 1 Section and reinforcement of frame beam and column.

Member	Story	Sectional dimension (mm×mm)	Arrangement of bars (C)
Frame column	1-3	700 × 700	1,625
	4-8	700 × 700	1,225
Frame beam	1-4	300 × 700	525
			422
	5-8	300 × 700	425
			322
Secondary beam	1-8	300 × 600	422
			322

analysis, the computational domain is also discretized along with the boundaries. To simplify the implementation of the viscoelastic artificial boundary, a centrally concentrated approach is utilized. As illustrated in Figure 1, coordinates X and Y represent the tangential directions, while Z represents the normal direction for the boundary.

The formulas for spring stiffness and damping coefficient are given by the following expressions:

$$K_1 = K_2 = \frac{2G}{R} \sum_{i=1}^4 A_i, \quad C_1 = C_2 \rho c_s \sum_{i=1}^n A_i \quad (2-1)$$

$$K_3 = \frac{4G}{R} \sum_{i=1}^4 A_i, \quad C_3 = \rho c_p \sum_{i=1}^n A_i \quad (2-2)$$

Where,

- ρ —Mass density;
- c_s —Shear wave velocity;
- c_p —Compressional wave velocity;
- G —Shear modulus;
- R —Distance from the wave source to the artificial boundary

The shear wave velocity and compressional wave velocity of the soil layers can be determined using the following formulas:

$$c_s = \sqrt{\frac{G}{\rho}} \quad (2-3)$$

$$c_p = \sqrt{\frac{\lambda + 2G}{\rho}} \quad (2-4)$$

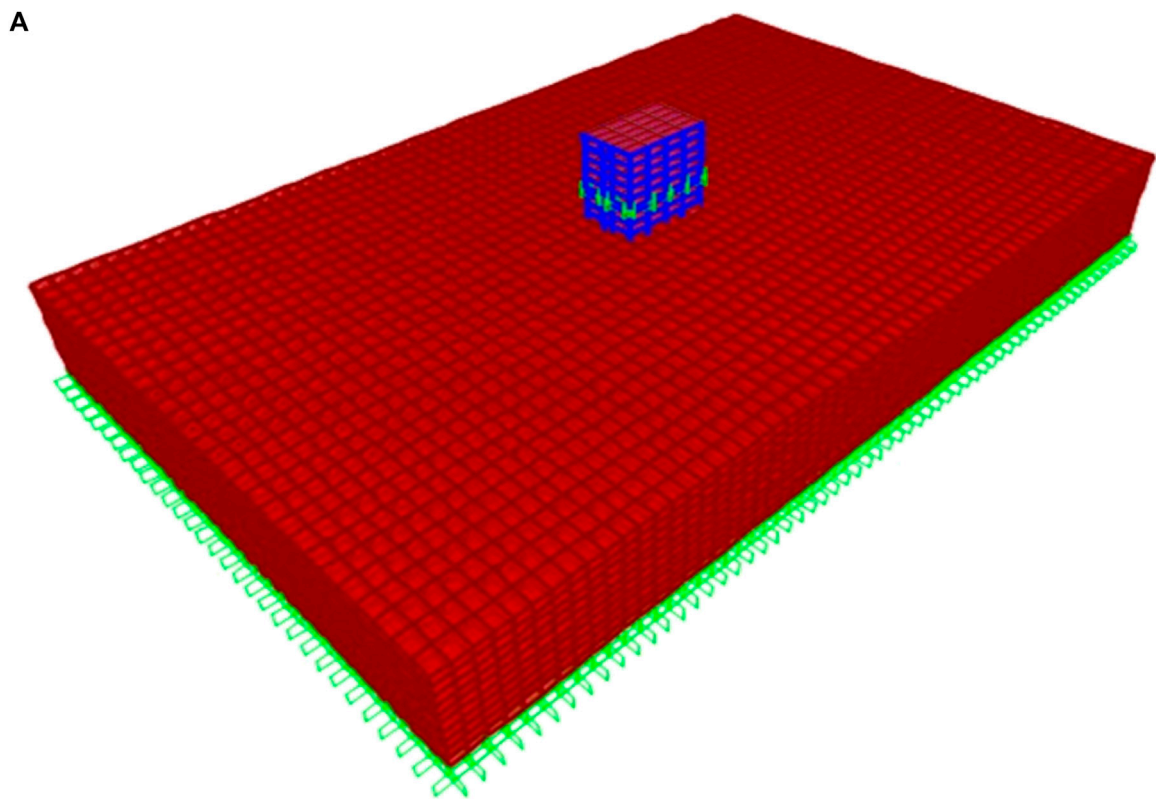
$$\lambda = \frac{E\mu}{(1 + \mu)(1 - 2\mu)} \quad (2-5)$$

Where,

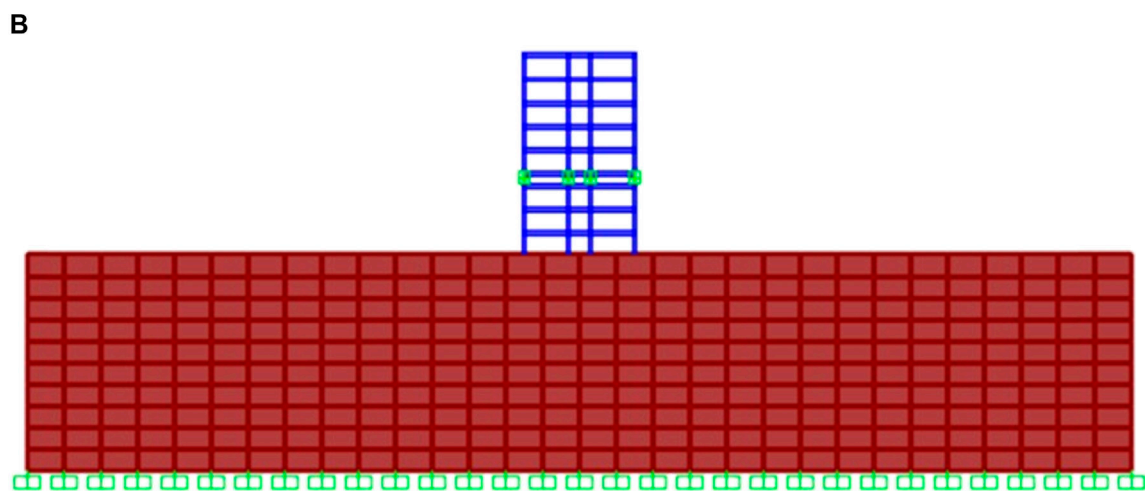
- μ —Poisson’s ratio;
- E —Elastic modulus;
- λ —Lamé constant, which remains consistent with the previous descriptions.

2.2 Project overview

An 8-story reinforced concrete frame structure is established with a seismic fortification intensity of 8° and a structural damping



Three-dimensional schematic of the structure considering SSI



Section of the structure considering SSI

FIGURE 2

Schematic diagram of the isolated structure considering the SSI effect. (A) Three-dimensional schematic of the structure considering SSI. (B) Section of the structure considering SSI.

ratio of 0.05. The isolation story is positioned at the top of the three stories. The building structure has a plane size of 24 m × 15 m, and each story has a height of 3.3 m. The slab thickness measures 150 mm, while the beam and slab have a concrete strength grade of C30. The column's concrete strength grade is C40, and the reinforcement is of strength grade HRB400 for the main bars

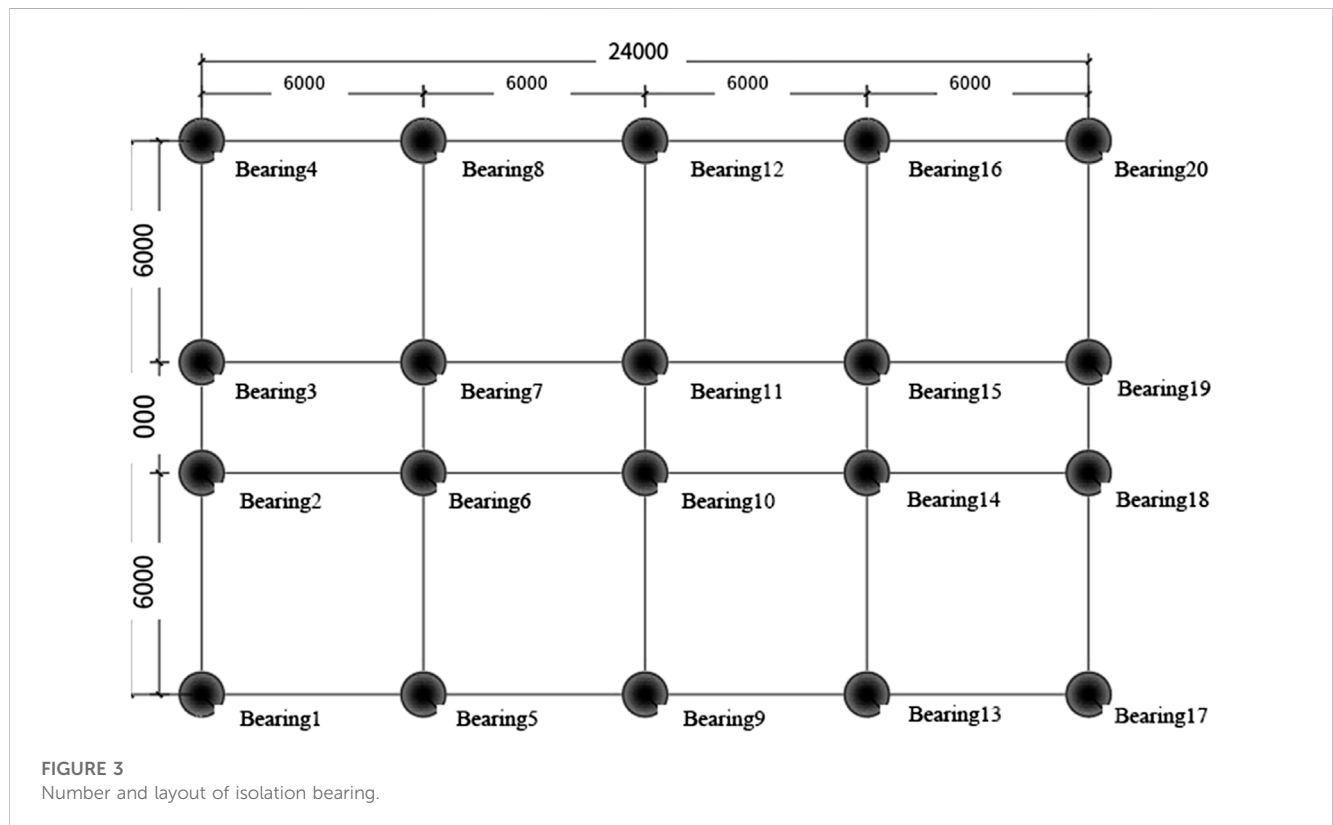
and HPB300 for the stirrups. The concrete cover has a thickness of 30 mm. Nonlinear material properties are assigned to the concrete with a strength grade of C40 using the Takeda hysteresis type. At the same time, HRB400 steel reinforcement is defined with the Kinematic hysteresis type. The frame columns are designated PMM plastic hinges, whereas the frame beams and beam

TABLE 2 (A) Parameters of foundation soil story.

Soil story name	Thickness (m)	Density (kg/m ³)	Poisson ratio	Shear modulus (10 ⁸ N/m ²)	Bulk modulus (10 ⁸ N/m ²)	Angle of internal friction (°)
Soft soil	3	2000	0.2	3.89	9.80	26
Medium soft soil	3	2,100	0.2	4.69	11.81	30
Hard soil	24	2,200	0.2	5.57	14.08	34

TABLE 3 Parameters of isolation bearing.

Model	Effective diameter	The total thickness of rubber (mm)	Initial shear stiffness (kN/m)	Equivalent stiffness (kN/m)	Vertical stiffness (kN/mm)	Yield force (kN)
LRB600	600	110	13,110	1,580	2,800	63.0



connections are labeled M3 plastic hinges. Table 1 provides detailed information on each story’s section dimensions and reinforcement of the beams and columns.

2.3 Modeling

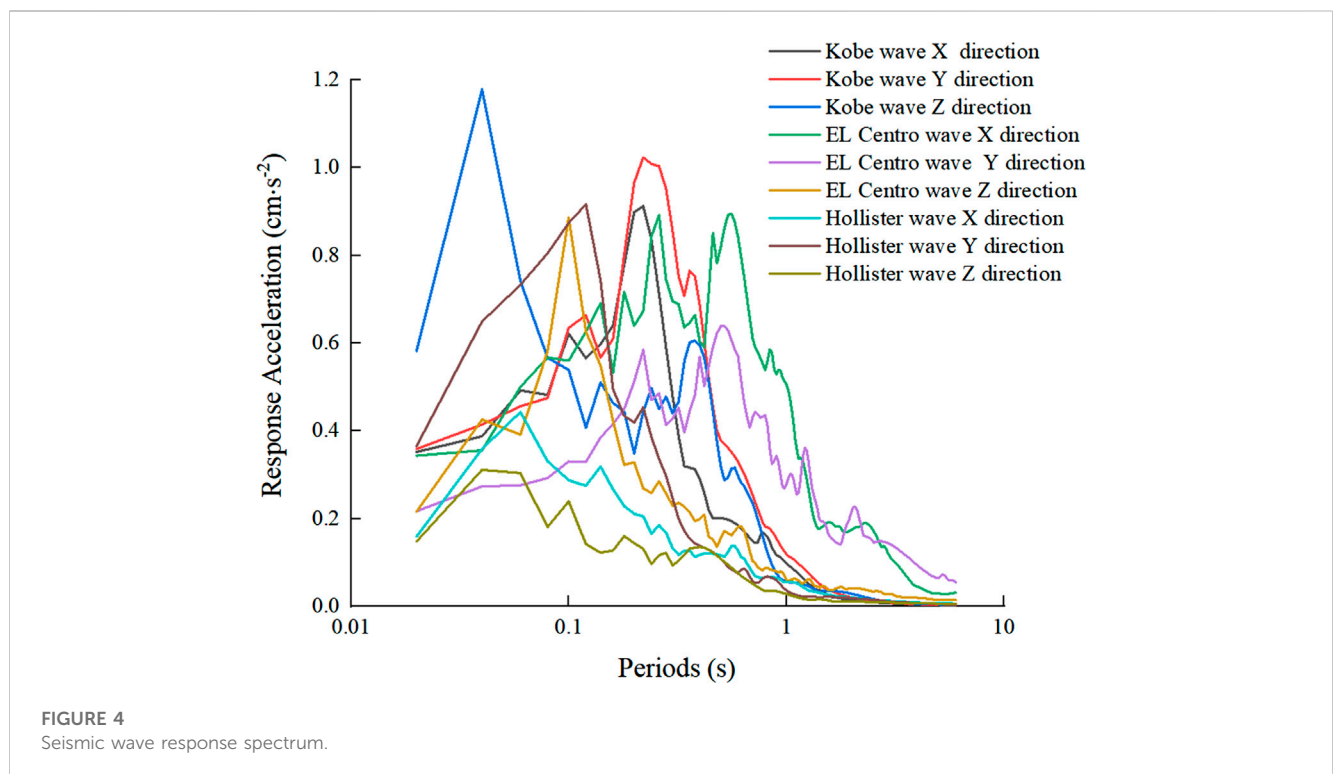
The finite element model of the inter-story isolation structure considering the SSI effect is established using SAP2000 software. Figure 2 illustrates the model, where the upper structure is simulated using frame elements, thick shell elements represent the raft foundation, and the foundation soil is modeled using solid

elements. The foundation size is ten times the structure size, with a plane size of 240 m × 150 m. The upper structure’s raft foundation is embedded in the soil layer, and a layered model with a thickness of 30 m is employed to capture the foundation soil’s characteristics better. Table 2 presents the parameters of the foundation soil, and an artificial viscoelastic boundary is set around the foundation soil boundary.

The SAP2000 software extracts the column bottom reaction *f* under the standard gravity load to determine the number and type of isolation support. The total horizontal yield force is estimated as 2% of the column bottom reaction under the standard gravity load, which helps determine the required isolation supports. The inter-

TABLE 4 Base-isolation seismic information Table.

Seismic wave name	Earthquake name	Time	Location	Focal depth/km	Magnitude	PGA/cm·s ⁻²
Kobe	Port Island	1995-01-16	Japan	17.9	6.9	289.8
						347.9
						566.8
El centro	Imperial valley	1940-05-19	California	8.8	6.9	210.1
						341.7
						206.4
Hollister	Hollister city hall annex	1974-11-28	California	6.1	5.2	174.6
						361.9
						193.2



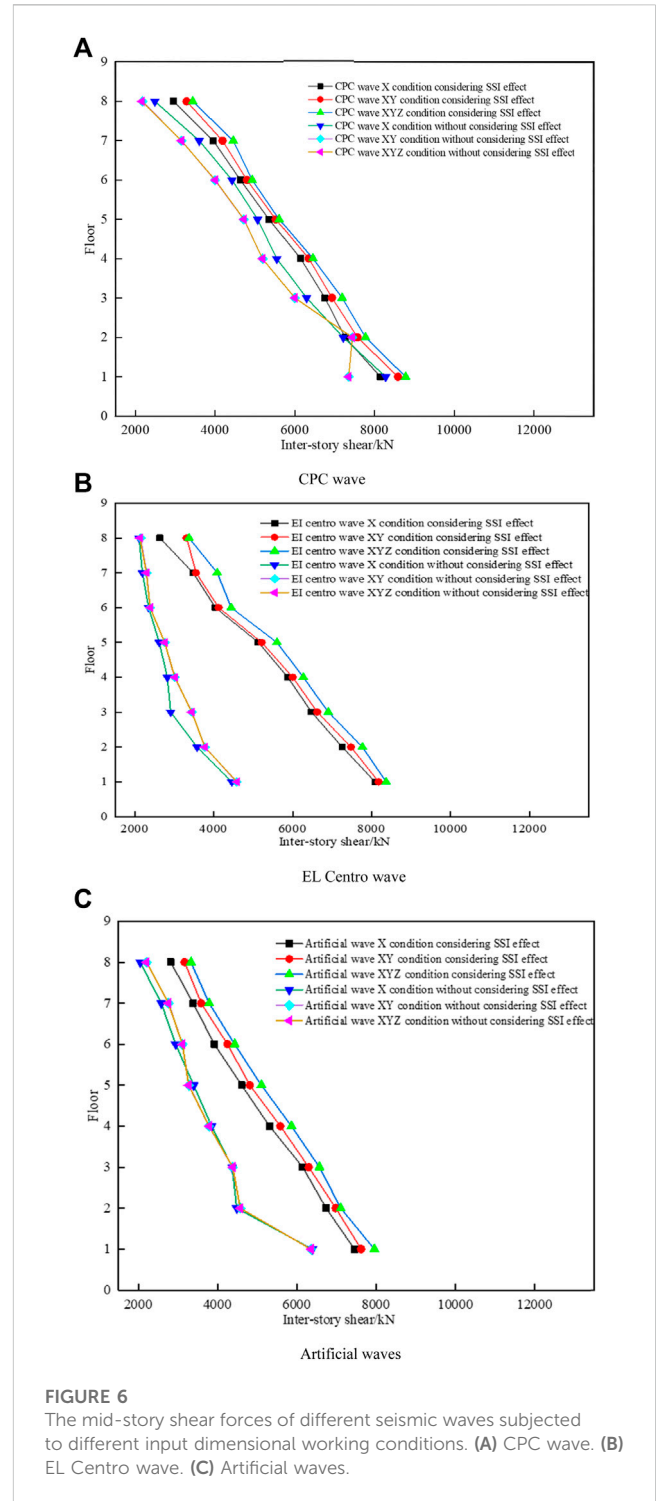
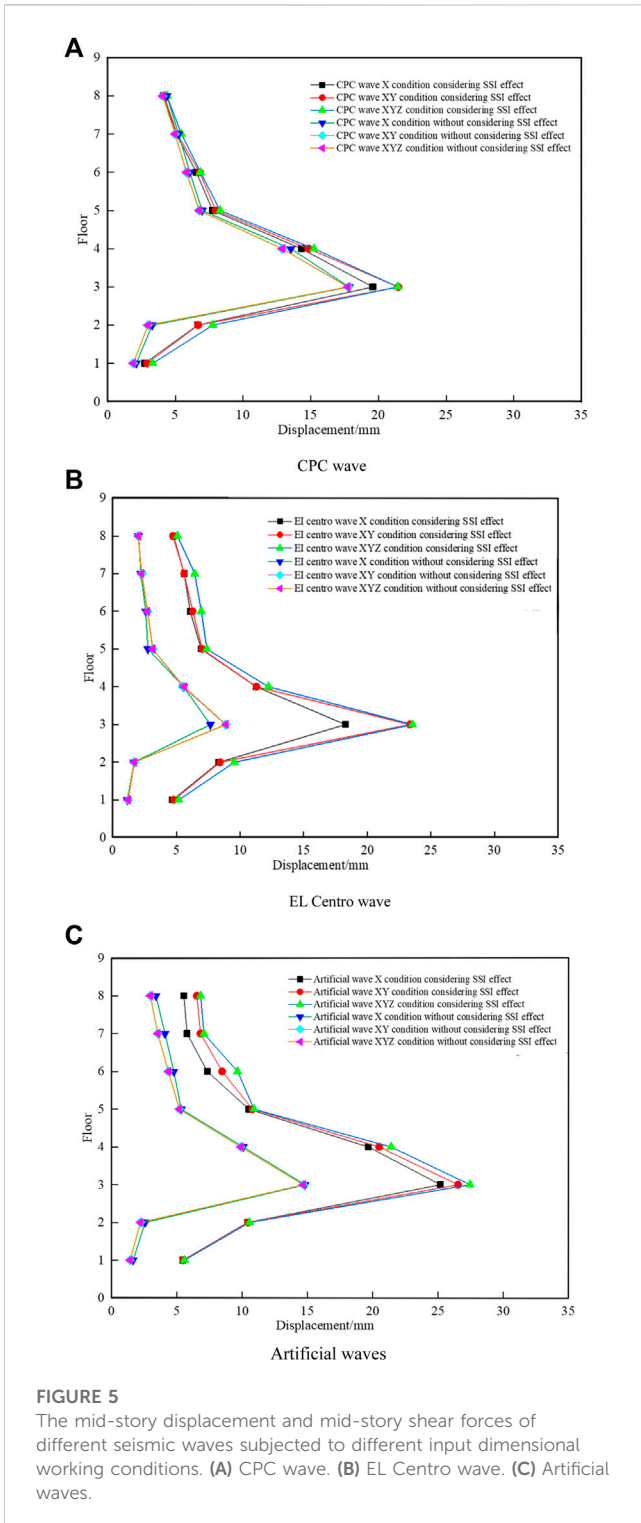
story isolation structure employs LRB600 isolation bearings; their parameters are listed in Table 3. The arrangement of the isolation bearings can be seen in Figure 3. The rubber isolator and gap elements are used in the isolation bearings to capture the vertical tension and compression nonlinear stiffness. To accurately represent the restoring force characteristics of the isolation story in the subsequent time history analysis, the Bouc-Wen model is employed.

2.4 Selection of seismic waves

This paper investigates the response of the inter-story isolation structure to three selected seismic waves. Table 4 provides the

ground motion information, while Figure 4 illustrates the acceleration response spectrum of these seismic waves. The maximum acceleration input of the three-dimensional seismic wave is adjusted based on the ratio of X direction, Y direction, and Z direction, set explicitly at 1:0.85:0.65. To align with the base-isolation seismic intensity of 8° during rare earthquakes, the peak acceleration of the seismic wave is adjusted to 400 cm/s².

The research on dynamic characteristics of isolated structures primarily focuses on inter-story displacement and inter-story shear. Assessing a building’s seismic capability involves examining the shear force variation between floors, which accurately reflects the seismic performance of each floor in the seismic isolation structure. To analyze the effects of soil-structure interaction (SSI), elastic-plastic time-history analysis is conducted on both staggered

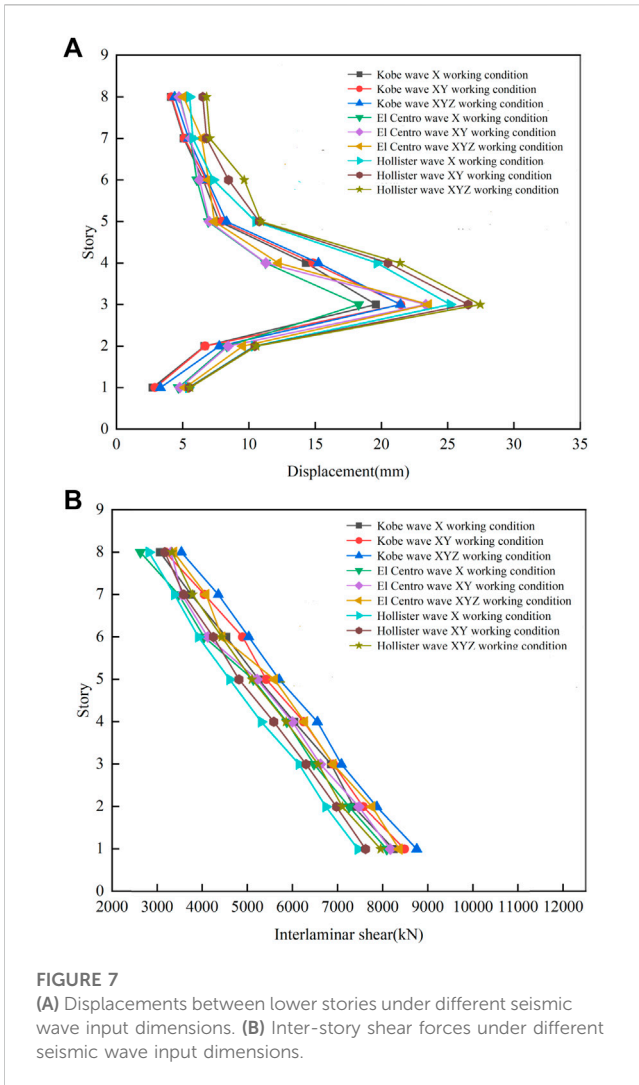


structures with and without SSI. Figure 6 compares inter-story displacement values between these two isolated structures.

Figure 5 reveals that the inter-story displacements of both types of inter-story isolated structures, subjected to three-dimensional seismic wave input, are greater than those under one-dimensional and two-dimensional seismic input. Additionally, considering the SSI effect, the inter-story seismic structure’s inter-story displacement values show more significant

variations across different seismic wave input dimensions compared to the results of the inter-story seismic structure without considering SSI.

Figure 6 compares inter-story shear values between the two isolated structures. It can be observed that the inter-story shear values of structures with varying story intervals under the influence of three-dimensional seismic wave input are consistently more extensive than those under one-dimensional and two-dimensional seismic inputs. Furthermore, the inter-



story shear value of the inter-story seismic structure considering the SSI effect is greater than that of the inter-story seismic structure without considering SSI across different seismic wave input conditions. Please refer to Figure 7 for a visual representation.

3 Seismic response analysis of inter-story isolation structure

3.1 Structural response analysis

An elastic-plastic time history analysis is conducted on the inter-story isolation structure, considering the SSI effect. The outcomes of story displacement and story shear are illustrated in Figures 7A, B, respectively. It is evident from both figures that when considering the SSI effect, the seismic response of the lower isolation structure under three-dimensional ground motion exhibits greater significance compared to that under one-dimensional and two-dimensional seismic inputs.

3.2 Response of the isolated bearing

Figure 8A illustrates the hysteresis curve of the recovery force-displacement for the isolation bearing subjected to underground motion input. The figure demonstrates that the hysteresis curve exhibits chaotic behavior when subjected to ground motion input. Along with the distinct hysteretic characteristics, it also displays specific viscous properties, indicating a correlation between the anisotropic responses following ground motion input. Consequently, the hysteresis curve of the support assumes an irregular shape. The restoring force model employed for the isolation bearing is depicted as a bilinear relationship, as illustrated in Figure 8B.

3.3 Isolation bearing analysis

In accordance with the seismic design code for buildings (Code for Seismic Design of Buildings, 2010), the maximum horizontal displacement of isolation bearings during rare earthquakes should not exceed the smaller value between 0.55 times the bearing diameter and three times the total thickness of rubber layers. For this study, LRB600 bearings are utilized, resulting in a horizontal displacement limit of 330 mm (600×0.55). Based on the time history analysis results, the maximum horizontal displacement of the inter-story isolation structure bearing, considering the SSI effect under different input conditions, is measured at 249.98 mm, which falls within the prescribed limit.

To ensure the effective performance of the inter-story isolation structure's bearings under an 8-degree rare earthquake, it is essential to evaluate both the tensile and compressive stress experienced by the approaches. As per the specifications, the tensile stress of the isolation bearing should not exceed 1 MPa, while the compressive stress should not exceed 30 MPa.

Figure 9A illustrates the compressive stress curve of the inter-story isolation structure's bearings. It is evident from the figure that the compressive stress generated by the Kobe and Hollister waves remains below 30 MPa. However, some bearings experienced compressive stress exceeding 30 MPa during the El Centro wave earthquake, and notably, bearing 18 exhibited the highest compressive stress, measuring 39.7 MPa, surpassing the specified limit.

The tensile stress curve of the bearings in the story isolation structure is presented in Figure 9B. Analysis of Figure 9B reveals that several bearings surpass the standard limit for tensile stress under each seismic wave. Notably, bearing 18 experienced maximum tensile stress of 2.2 MPa during the Kobe wave earthquake, exceeding the standard limit by more than twice. Similarly, under the El Centro wave earthquake, bearing 15 reaches a maximum tensile stress of 1.4 MPa, while under the Hollister wave earthquake, support 15 exhibits an ultimate tensile stress of 1.5 MPa.

Based on the analysis of the bearing stress curve, it can be concluded that when considering the SSI effect under three-dimensional ground motion, the conventional horizontal isolation bearing used in the story isolation structure fails to isolate vertical ground motion effectively. Furthermore, specific bearings encounter issues of tensile and compressive stress exceeding the limits. To address this problem, the implementation of a vertical isolation device is proposed.

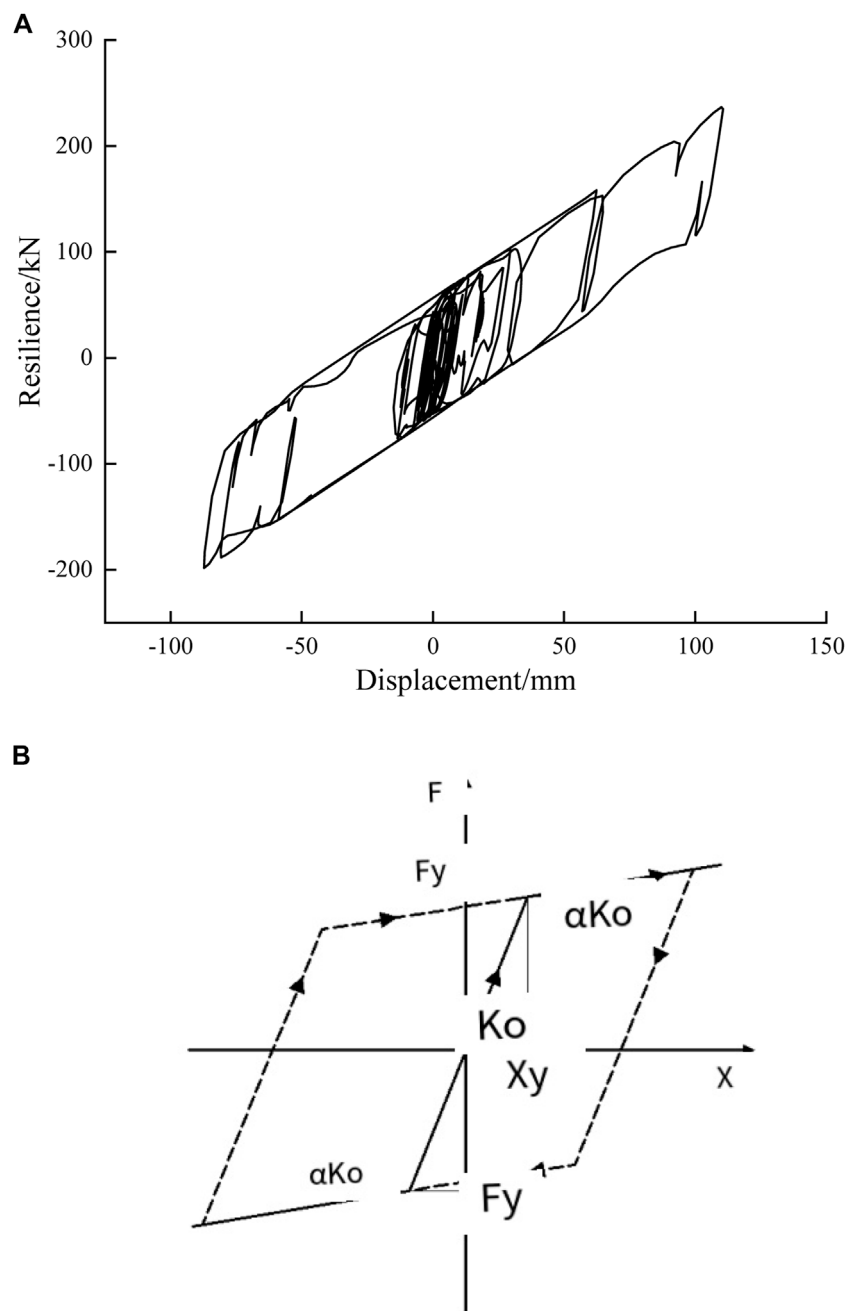


FIGURE 8 (A) Force-displacement hysteresis curve. (B) Recovery force model of isolation bearing.

4 Seismic response analysis of inter-story isolation structure with three-dimensional isolation bearing

4.1 Three-dimensional isolation bearing modeling

A three-dimensional isolation structure model incorporating a vertical isolation bearing is constructed in this study. For the vertical isolation story, a steel spring with a stiffness of 8×10^3 kN/m is chosen as the vertical isolation bearing. It is complemented by

parallel viscous dampers, represented by the Damper element. The seismic response of traditional horizontal and three-dimensional isolation structures is compared and analyzed under three-dimensional ground motion excitations.

4.2 Modal analysis

Modal analysis is performed on both the three-dimensional and traditional horizontal isolation structures, and the results for the first six natural vibration periods are presented in Table 5. It is evident

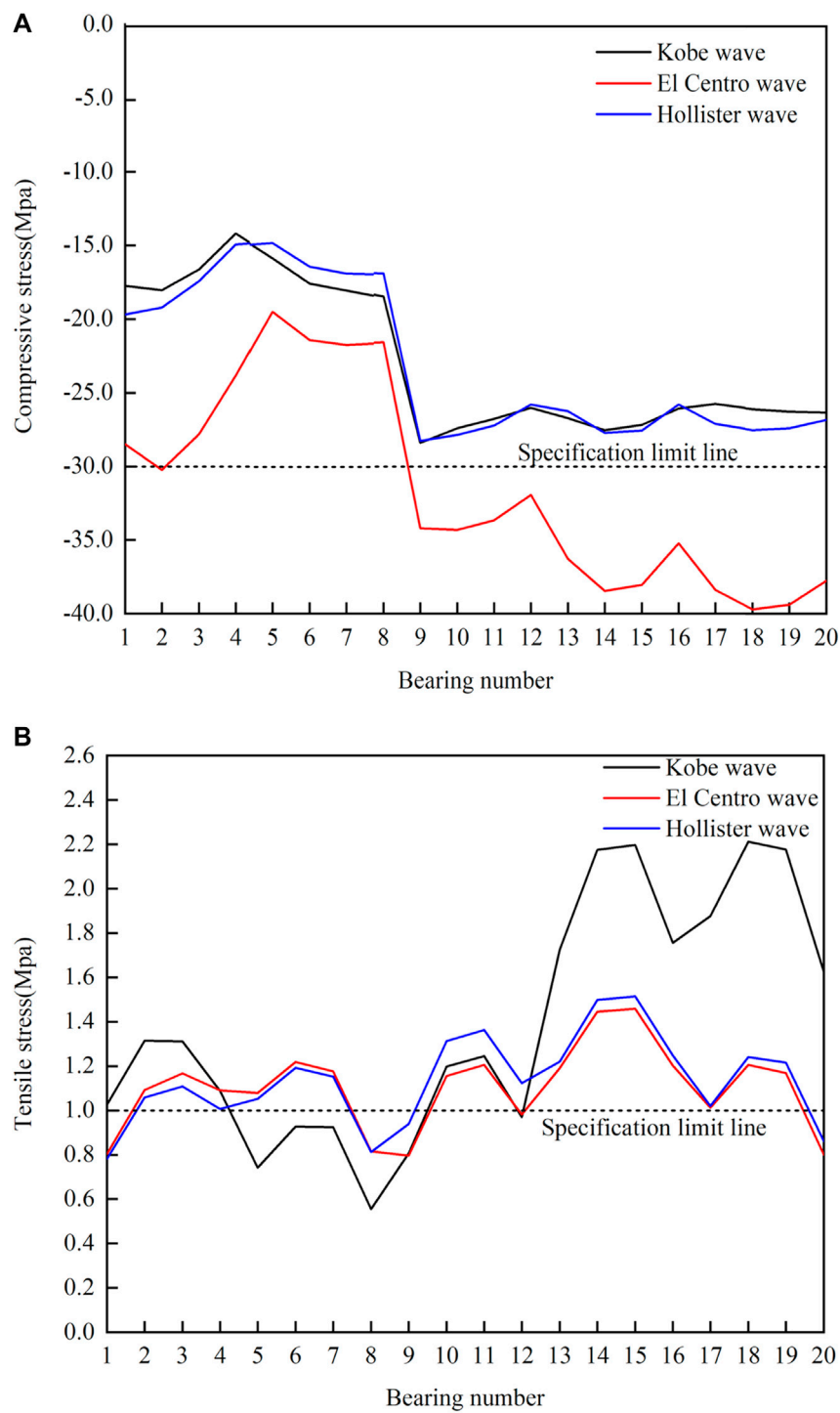


FIGURE 9
(A) Compression stress curve of isolation bearing. **(B)** Tensile stress curve of isolation bearing.

from Table 5 that the three-dimensional isolation structure exhibits longer natural vibration periods compared to the traditional horizontal isolation structure. This can be attributed to the presence of an additional vertical isolation device in the three-dimensional structure, which enhances the system’s flexibility and further extends the natural vibration period of the structure.

Moreover, the three-dimensional isolation structure’s fourth, fifth, and sixth modes experience a more pronounced increase in their natural vibration periods when compared to the traditional horizontal isolation structure. This significant extension of the natural vibration periods for these modes contributes to an enhanced damping effect within the isolation structure, particularly for the respective methods mentioned.

TABLE 5 Natural vibration periods of different isolated structures (s).

Mode order	Traditional horizontal isolation structure	Three-dimensional seismic isolation structure
1	3.064	3.161
2	3.025	3.143
3	2.878	2.898
4	0.475	0.685
5	0.425	0.651
6	0.421	0.634

TABLE 6 Comparison of maximum displacement between different isolation structures under different seismic input conditions (mm).

Seismic wave	Input direction	Traditional horizontal isolation structure	Three-dimensional seismic isolation structure
Kobe wave	X	19.59	21.45
	XY	21.47	22.28
	XYZ	21.44	23.35
El centro wave	X	18.28	19.29
	XY	23.35	25.16
	XYZ	23.57	25.40
Hollister wave	X	25.20	26.02
	XY	26.54	26.41
	XYZ	27.46	28.58

4.3 Isolation effect analysis

4.3.1 Displacement comparison

The maximum inter-story displacement of the three-dimensional isolation structure is compared to that of the traditional horizontal isolation structure, and the results are presented in Table 6. The findings in Table 6 reveal that the additional three-dimensional isolation bearing leads to a more significant displacement in the isolation story, particularly noticeable when subjected to three-dimensional ground motion.

The maximum horizontal displacement of the three-dimensional seismic isolation structure under various input conditions is measured at 306.49 mm. While this value exceeds the displacement observed in the traditional horizontal isolation structure, it remains within the acceptable limit specified by the regulations.

4.3.2 Base shear comparison

The comparison of base shear between the three-dimensional isolation structure and the traditional horizontal isolation structure under three-dimensional seismic input is depicted in Figure 10A. As observed in Figure 10A, the base shear force of the three-dimensional isolation structure is smaller than that of the traditional horizontal isolation structure when subjected to seismic waves. This observation indicates that the presence of the

vertical isolation device helps further attenuate the energy transmitted to the superstructure.

4.3.3 Vertex vertical acceleration comparison

The comparison of vertical acceleration between the three-dimensional seismic isolation structure and the traditional horizontal seismic isolation structure under three-dimensional seismic input is presented in Figure 10B. Figure 10B shows that the three-dimensional seismic isolation structure exhibits superior control over the vertical acceleration of the vertex compared to the traditional horizontal seismic isolation structure. The three-dimensional seismic isolation approach effectively mitigates the vertical acceleration at the top of the structure, thereby minimizing the transmission of vertical seismic forces to the upper structure and demonstrating an excellent vertical isolation effect.

4.4 Stress comparison of isolation bearing

The bearing pressure stress curve of the three-dimensional isolation structure is illustrated in Figure 11A. It is evident from Figure 11A that the maximum compressive stress experienced by the three-dimensional isolated structure under different seismic waves is 28.9 MPa, which is below the allowable limit specified in the code.

Figure 11B depicts the tensile stress of the isolation bearing. Figure 11B shows that the maximum tensile stress of the

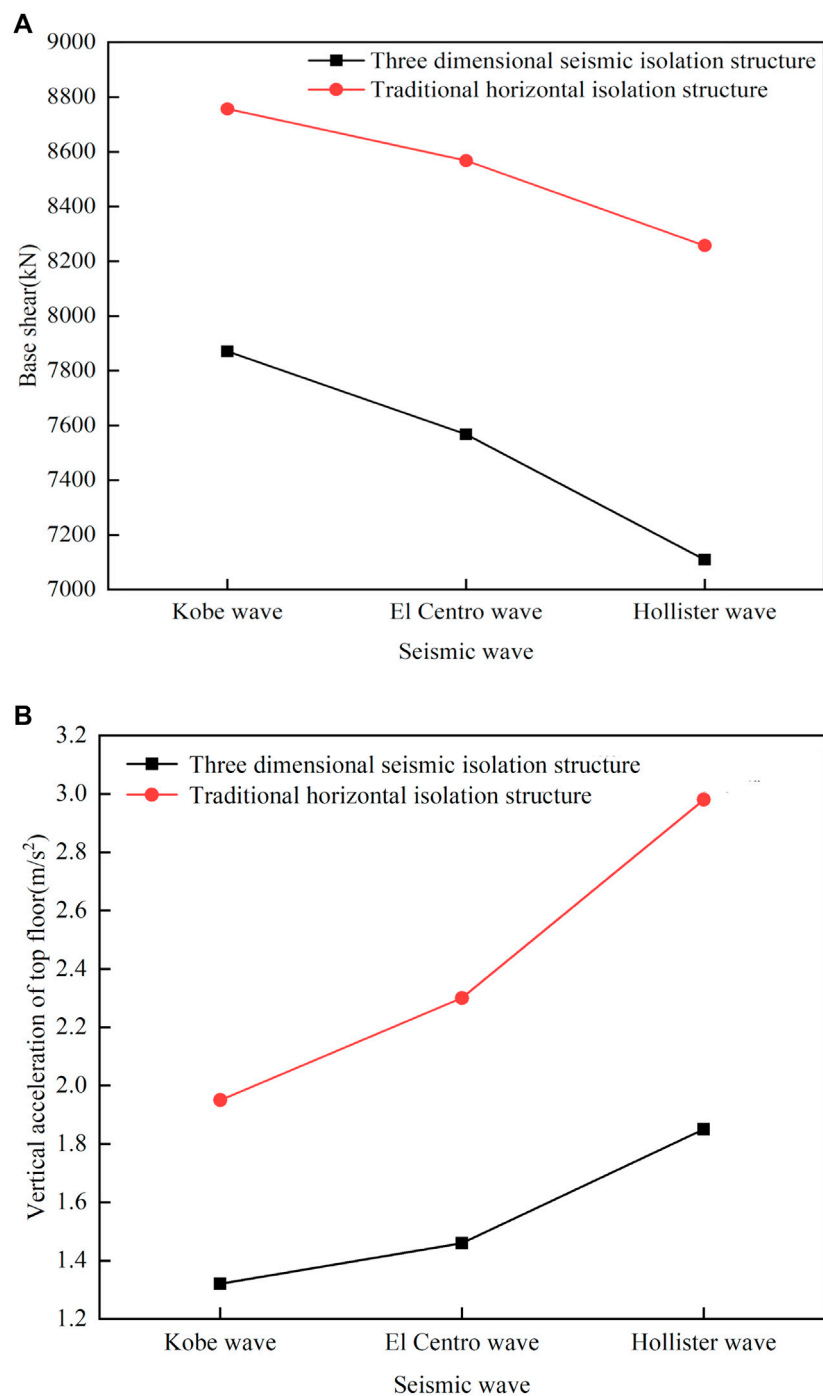


FIGURE 10
(A) Base shear force under XYZ seismic waves. **(B)** Vertical acceleration of top floor under XYZ seismic waves.

three-dimensional isolation structure under various seismic waves is 0.9 MPa, lower than the ultimate tensile stress the specifications allow. Furthermore, the maximum tensile stress of the bearing after incorporating the vertical isolation device is reduced by 59% compared to the maximum tensile stress of the isolation bearing in the traditional horizontal isolation structure. This optimization of stress in isolation bearing effectively addresses the issue of tensile stress exceeding limits in the conventional horizontal isolation

structure under three-dimensional ground motion, thereby achieving the desired damping effect.

4.5 Stress comparison of foundation soil

A three-dimensional isolation structure’s effectiveness lies in its superior damping effect and in considering the stress imposed

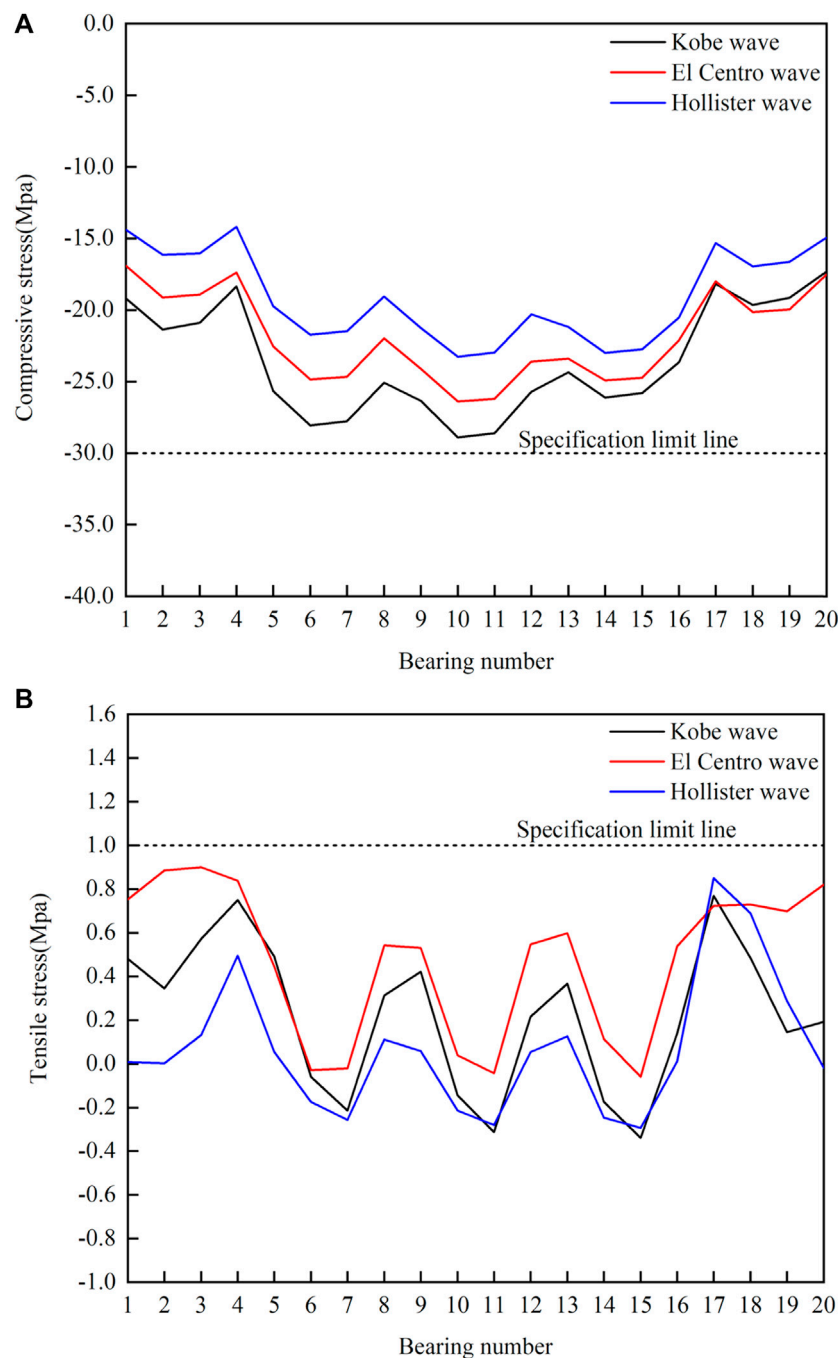


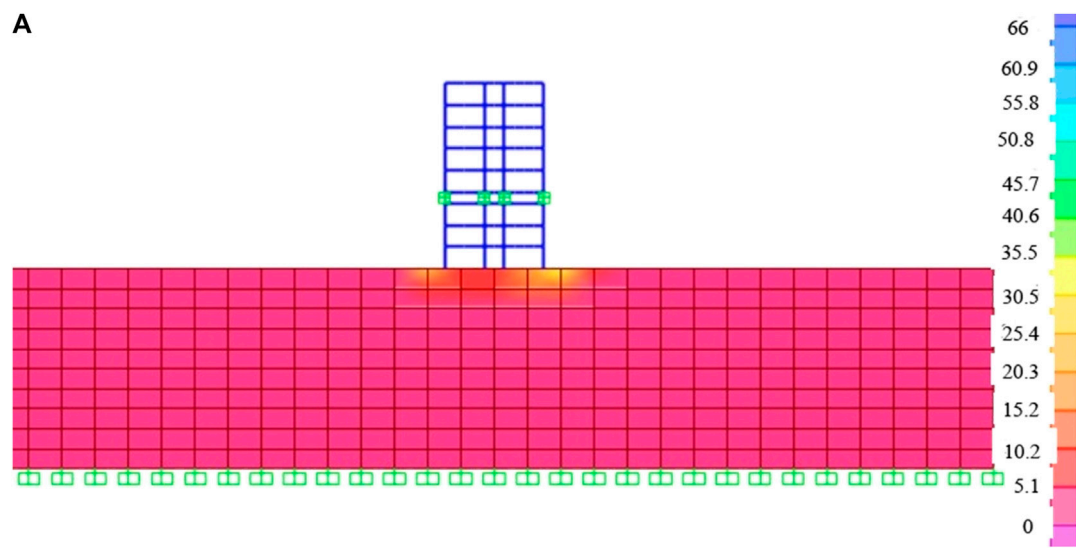
FIGURE 11
(A) Compression stress curve of isolation bearing for three-dimensional isolated structure. **(B)** Tensile stress curve of three-dimensional isolation structure isolation bearing.

on the foundation soil as a crucial criterion for evaluating its overall isolation performance. Figure 12 illustrates the comparison of the maximum soil stress between the two isolation structures under three-dimensional ground motion input. As depicted in Figure 12, incorporating the three-dimensional isolation bearing results in lower soil stress on the foundation than the traditional horizontal isolation bearing. Reducing soil stress is advantageous for the foundation and facilitates better design.

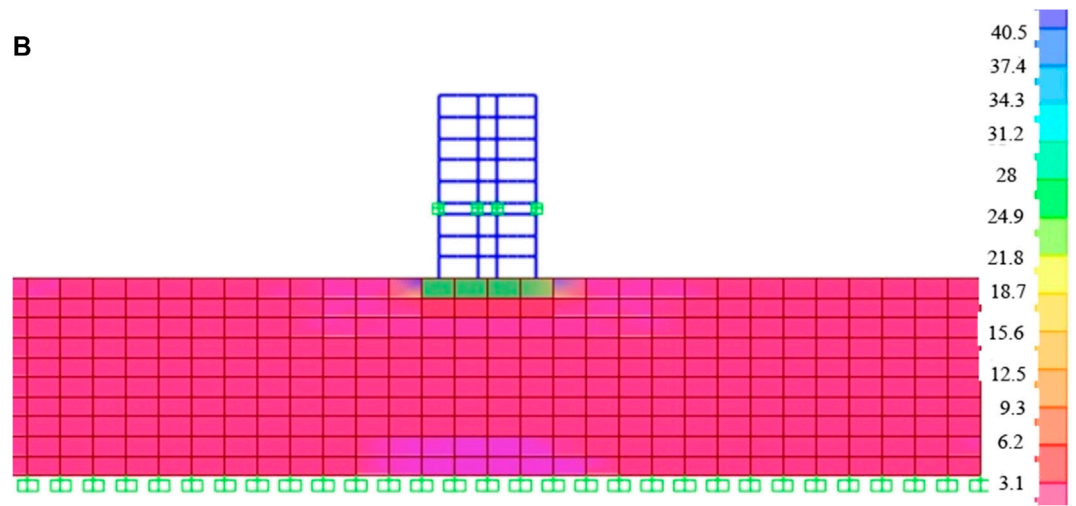
5 Analysis and comparison of the response of inter-story seismic structures considering SSI effect in different soil stories to 3D earthquakes

5.1 Setting of different soil stories

Based on the soil characteristics of the stories, two distinct sites are established in the inter-story seismic model that



Soil stress diagram of traditional horizontal isolation structure

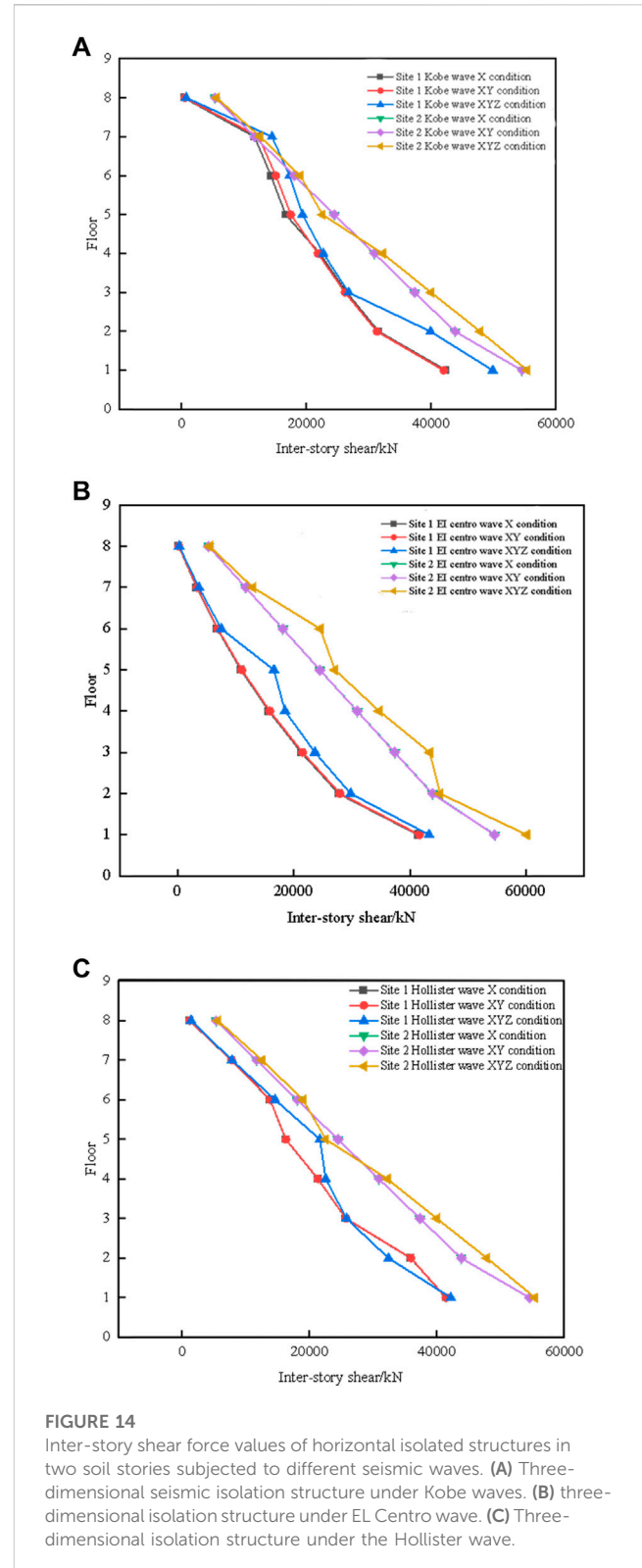
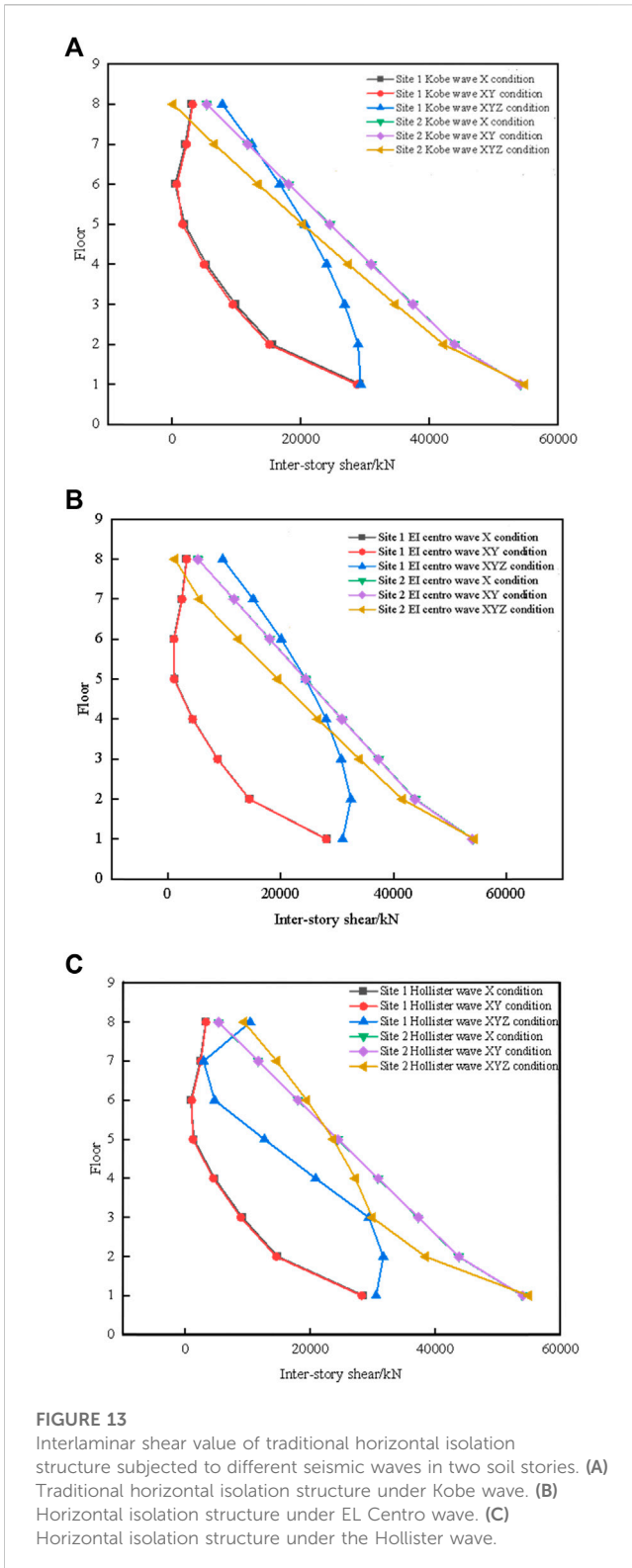


Soil stress diagram of the three-dimensional isolated structure

FIGURE 12 Comparison of soil stress of two isolation structures. (A) Soil stress diagram of traditional horizontal isolation structure. (B) Soil stress diagram of the three-dimensional isolated structure.

TABLE 7 Different soil parameters.

Site number	Soil story properties	Soil story number	Soil story thickness (m)	Shear modulus (Mpa)	Modulus of elasticity (Mpa)	Poisson's ratio	Shear wave velocity (m/s)
Site 1	Hard soil	1	3	125	325	0.3	250
		2	3	259.2	622.1	0.2	360
		3	24	445.5	1,069.2	0.2	450
Site 2	Soft soil	1	3	14.6	40.8	0.4	90
		2	3	58.3	151.6	0.3	180
		3	24	352.8	846.7	0.2	420



accounts for the soil-structure interaction (SSI) effect. Site 1 represents hard soil, while Site 2 represents soft soil. The selected parameters for the soils at these two sites are presented in Table 7. The subsequent analysis focuses on

examining the disparity in response and isolation effectiveness between traditional horizontal isolation structures and three-dimensional isolation structures when considering the SSI effect at each site.

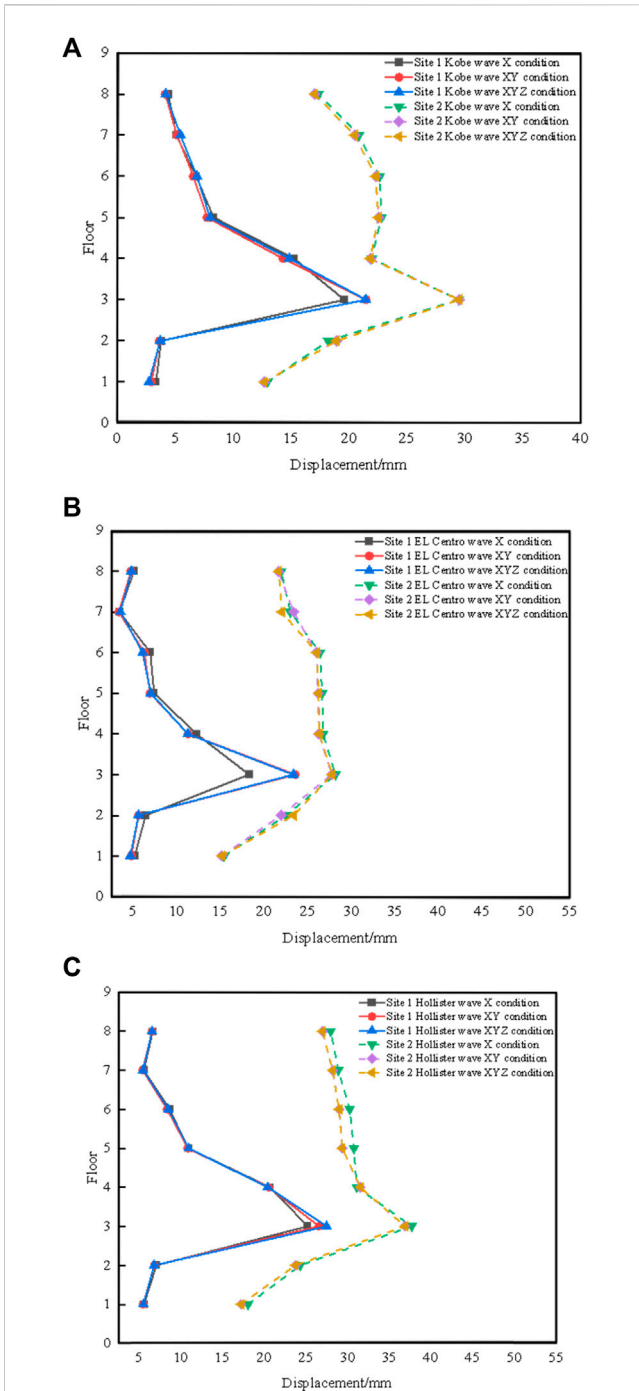


FIGURE 15
Inter-story displacement of horizontal isolation structure subjected to different seismic waves. (A) Traditional horizontal isolation structure under Kobe wave. (B) Traditional horizontal isolation structure under EL Centro wave. (C) Traditional horizontal isolation structure under the Hollister wave.

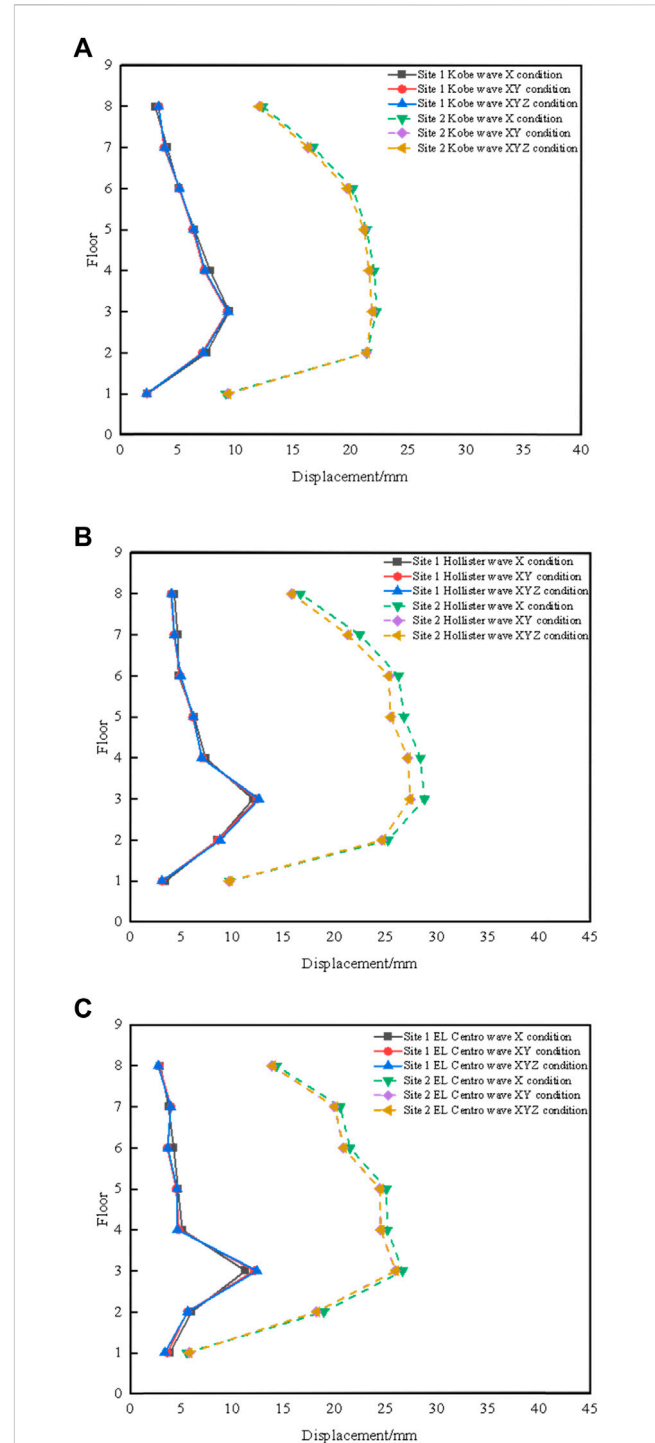


FIGURE 16
The inter-story displacement values of three-dimensional isolated structures subjected to different seismic waves in two soil stories. (A) Three-dimensional seismic isolation structure under Kobe waves. (B) three-dimensional isolation structure under EL Centro wave. (C) Horizontal isolation structure under the Hollister wave.

5.2 Comparative analysis of the structural response

5.2.1 Comparative analysis of shear forces between stories

Based on the results obtained from the time history analysis, the inter-story shear forces of both traditional horizontal

isolation structures and three-dimensional isolation structures were investigated under different soil stories. The inter-story shear forces of the horizontal isolation structures, accounting for the soil-structure interaction (SSI) effect, are depicted in Figure 13. As observed in Figure 13, the inter-story shear

TABLE 8 Maximum vertex acceleration of traditional horizontal isolation structure subjected to different seismic wave inputs in different soil stories (m·s⁻²).

Seismic wave input condition	Site 1	Field 2	Field 2/Field 1
Kobe wave X condition	4.06	7.17	1.77
Kobe wave XY condition	3.71	6.96	1.88
Kobe waves XYZ condition	3.34	6.94	2.08
Hollister wave X condition	7.46	10.33	1.38
Hollister wave XY condition	6.99	10.10	1.44
Hollister wave XYZ condition	6.83	10.02	1.47
EL centro wave X condition	6.27	9.54	1.52
EL centro wave XY condition	5.72	9.38	1.64
EL centro wave XYZ condition	5.66	9.39	1.66

value of the traditional horizontal isolation structure, considering the SSI effect at site 2, surpasses that at site 1 under the same multi-dimensional seismic input conditions. Similarly, Figure 14 illustrates the inter-story shear of the three-dimensional seismic isolation structure, incorporating the SSI effect, for different soil stories. It is evident from Figure 14 that, like the traditional horizontal isolation structure, the inter-story shear value of the three-dimensional isolation structure, considering the SSI effect at site 2, exceeds that at site 1 under the same multi-dimensional seismic input conditions. The findings from Figures 13, 14 demonstrate that both the horizontal isolation structure and three-dimensional isolation structure, considering the SSI effect, result in larger shear forces in the soft soil story compared to the hard soil story.

5.2.2 Comparative analysis of inter-story displacement

Based on the results obtained from the time history analysis, the inter-story displacements of two types of isolation structures were extracted under different soil stories. Figure 15 illustrates a comparison of the inter-story displacements of traditional horizontal isolation structures under different soil stories, considering the soil-structure interaction (SSI) effect. As depicted in Figure 15, the horizontal isolation structure at site 2, regarding the SSI effect, exhibits significantly larger inter-story displacement values than at site 1 under the same multi-dimensional seismic input conditions. Similarly, Figure 16 displays the inter-story displacements of three-dimensional seismic isolation structures considering the SSI effect for different soil stories. It can be observed from Figure 16 that, akin to the horizontal isolation structure, the three-dimensional isolation structure considering the SSI effect at site 2, still demonstrates greater inter-story displacement than at site 1 under the same multi-dimensional seismic input conditions. Combining the findings from Figures 15, 16, it becomes evident that both the horizontal isolation structure and three-dimensional isolation structure, considering the SSI effect, generate larger inter-story displacements in soft soil compared to hard soil. Furthermore, when considering different isolation

structures with the SSI effect, it is noted that the softer the soil story, the greater the structural displacement response.

5.3 Comparative analysis of isolation effect

5.3.1 Comparative analysis of vertex acceleration

Table 8 present the vertex acceleration values for the traditional horizontal and three-dimensional isolation structures. The data indicate that both structures exhibit significantly higher vertex accelerations on the soft soil story at site 2 compared to the isolation structure on the complex soil story. Notably, the three-dimensional isolation structure shows a greater increase in vertex acceleration on the soft soil story than the horizontal isolation structure. These findings suggest that the isolation effect of the three-dimensional structure is less pronounced on the soft soil story in comparison to the hard soil story.

5.3.2 Comparative analysis of support stress

The bearing stress envelope values of three seismic wave time histories were analyzed to investigate the influence of soil story properties on the isolation effect of both the traditional horizontal isolation structure and the three-dimensional isolation structure. These structures' tensile and compressive stress values were compared and examined on different soil stories. The results of the tensile stress comparison are presented in Figure 17A, while Figure 17B illustrates the compressive stress comparison. As depicted in Figure 17A, the tensile stress experienced by the supports of the same isolation structure on the soft soil story at site 2 is significantly higher than that at site 1. The traditional horizontal isolation structure exhibits tensile stress exceeding the limit on both soil stories at site 1 and site 2. Meanwhile, the three-dimensional isolation structure shows no tensile stress exceeding the limit at site 1 but does encounter this issue on the soft soil story. Turning to Figure 17B, it is evident that the compressive stress experienced by both the traditional horizontal isolation structure and the three-dimensional isolation structure is greater on the soft soil story at site 2 compared to site 1. However, the compressive stress values for both structures remain within acceptable limits.

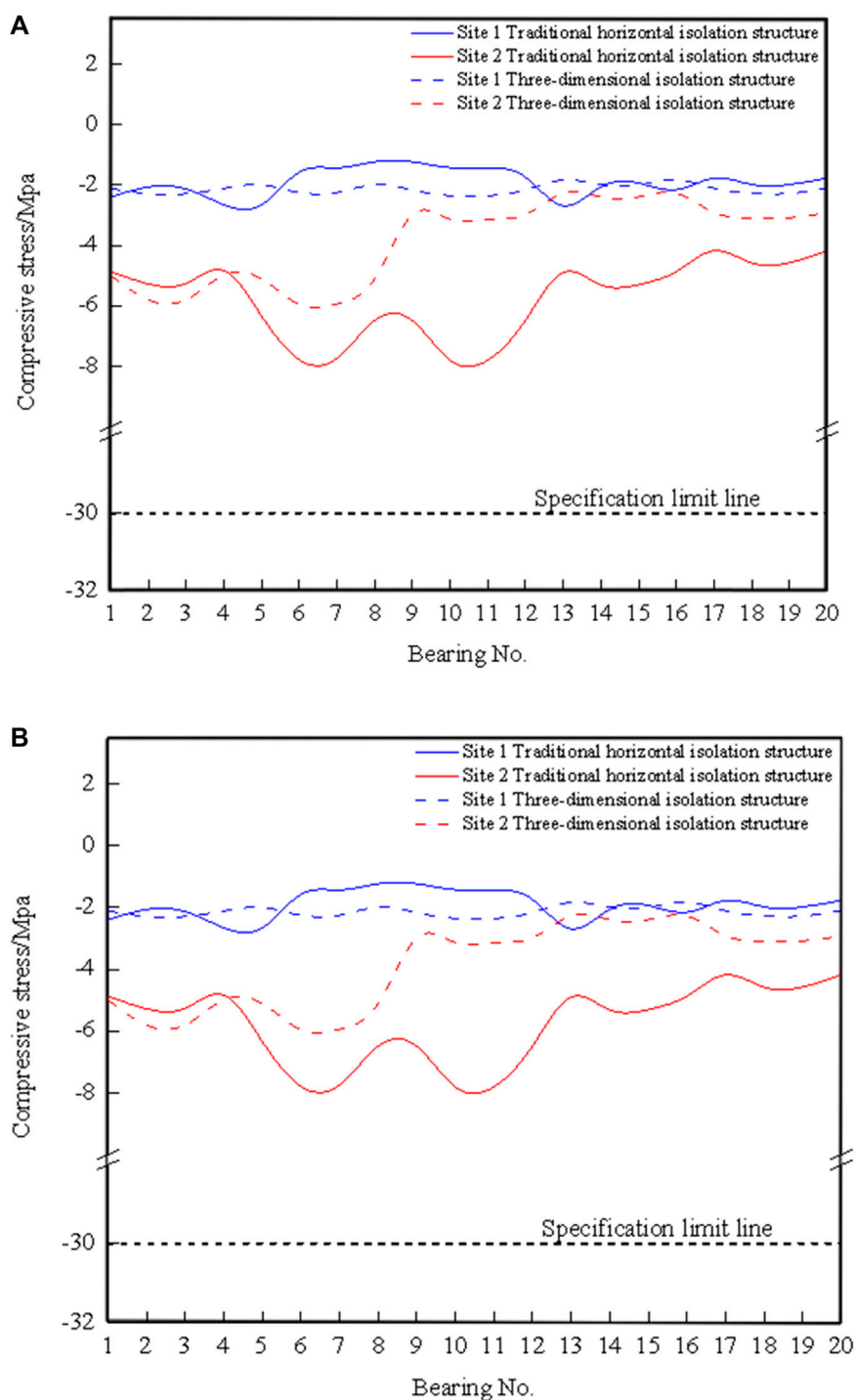


FIGURE 17

(A) Tensile stress of isolation structure bearing in different soil stories. (B) Bearing Pressure Stress of Isolated Structures in Different Soil Stories.

6 Conclusion and discussion

6.1 Conclusion

This paper establishes an inter-story isolation structure model considering the soil-structure interaction (SSI) effect. Various

ground motion scenarios, including one-dimensional, two-dimensional, and three-dimensional inputs, are applied to compare the seismic responses of inter-story isolation structures. A three-dimensional isolation device is introduced to address the issue of tensile and compressive stress exceeding the limits in isolation bearings under three-dimensional seismic input. The

seismic response results of traditional horizontal isolation structures are analyzed and compared. The following conclusions are drawn from the study.

- (1) considering the SSI effect, the inter-story isolation structure exhibits larger inter-story displacement and inter-story shear values than the two-dimensional and one-dimensional seismic inputs under three-dimensional seismic conditions.
- (2) The inclusion of three-dimensional isolation bearings in the three-dimensional isolation structure effectively reduces the transmission of vertical seismic waves to the upper structure, thereby achieving excellent vertical isolation.
- (3) The use of three-dimensional isolation significantly mitigates the tension and compression stress in the isolation structure bearings, effectively addressing the issue of excessive stress observed in traditional horizontal isolation structures under three-dimensional seismic actions. This optimization of bearing forces results in the expected damping effect.
- (4) The introduction of three-dimensional isolation bearings leads to lower soil stress in the foundation compared to the traditional horizontal isolation bearings, which has positive implications for foundation design considerations.

6.2 Discussion

Inter-story isolation, as an emerging seismic isolation technology, has been implemented in numerous inter-story isolation engineering examples both domestically and internationally. However, the theoretical framework for this system is still not sufficiently developed, and the relevant literature is relatively scarce. Furthermore, there has been no research on inter-story isolation considering the Soil-Structure Interaction (SSI) effects under three-dimensional seismic conditions. This paper focuses on the response of inter-story isolated structures considering SSI effects during three-dimensional seismic events. Numerical simulation analysis is conducted to investigate the seismic response under four influencing factors: SSI effects, the dimension of seismic input, the type of seismic input, and the type of isolation bearings. Modal analysis and time-history analysis are employed for seismic response comparison. The impact of both stiff and soft soil layers on the response of inter-story isolated structures considering SSI effects under three-dimensional seismic input conditions is explored, offering valuable insights for further in-depth research on inter-story isolation structures.

In comparison to base isolation, inter-story isolation may lead to severe consequences and significant losses if the isolation layers are damaged, potentially resulting in the overall collapse of the

superstructure. Thus, further exploration and protection measures regarding the performance requirements of isolation layers are necessary. The scope of this study is limited to the response of regular framed inter-story isolation structures considering SSI effects. If the structural configuration is altered, the response of irregular structures with inter-story isolation under three-dimensional seismic conditions and their effectiveness in reducing seismic effects warrant further investigation. Additionally, the seismic input for inter-story isolation structures consists of two horizontal components and one vertical component. However, real seismic effects also include torsional components, and it remains a subject of further research to examine the changes in response patterns when considering torsional effects in inter-story isolated structures.

Data availability statement

The original contributions presented in the study are included in the article/supplementary material, further inquiries can be directed to the corresponding authors.

Author contributions

JX: Data curation, Software, Writing—original draft. HG: Writing—review and editing. ZiG: Data curation, Writing—review and editing. JZ: Software, Writing—original draft. ZY: Data curation, Writing—review and editing. GZ: Writing—review and editing. ZhG: Methodology, Writing—review and editing. DL: Methodology, Writing—review and editing. WS: Writing—review and editing.

Conflict of interest

The authors declare that the research was conducted in the absence of any commercial or financial relationships that could be construed as a potential conflict of interest.

Publisher's note

All claims expressed in this article are solely those of the authors and do not necessarily represent those of their affiliated organizations, or those of the publisher, the editors and the reviewers. Any product that may be evaluated in this article, or claim that may be made by its manufacturer, is not guaranteed or endorsed by the publisher.

References

- Basili, M., and Angelis, M. D. (2022). Experimental dynamic response of a multi-story frame structure equipped with non-conventional TMD implemented via inter-story isolation. *Appl. Sci.* 12 (18), 9153. doi:10.3390/app12189153
- Bernardi, E., Donà, M., and Tan, P. (2023). Multi-objective optimization of the inter-story isolation system used as a structural TMD. *Bull. Earthq. Eng.* 21 (5), 3041–3065. doi:10.1007/s10518-022-01592-9
- Bolvardi, V., Pei, S., van de Lindt, J. W., and Dolan, J. D. (2018). Direct displacement design of tall cross-laminated timber platform buildings with inter-story isolation. *Eng. Struct.* 167, 740–749. doi:10.1016/j.engstruct.2017.09.054
- Davide, F., and Kalfas Konstantinos, N. (2023). Inter-story seismic isolation for Figure-rise buildings. *Eng. Struct.* doi:10.1016/J.ENGSTRUCT.2022.115175

- Ehsan, G., and Toopchi-Nezhad, H. (2023). Annular fiber-reinforced elastomeric bearings for seismic isolation of lightweight structures. *Soil Dyn. Earthq. Eng.* 166, 107764. doi:10.1016/j.soildyn.2023.107764
- Faiella, D., Calderoni, B., and Mele, E. (2022). Seismic retrofit of existing masonry buildings through inter-story isolation system: a case study and general design criteria. *J. Earthq. Eng.* 26 (4), 2051–2087. doi:10.1080/13632469.2020.1752854
- Fan, Y., Liu, D., Lei, M., Zheng, Y., Zhao, T., and Gao, L. (2023). Seismic fragility analysis of the inter-story isolated structure for the influence of main-aftershock sequences. *Adv. Mech. Eng.* 1, 168781322211457. doi:10.1177/16878132221145791
- Gao, Y., Yu, Z., Chen, W., Yin, Q., Wu, J., and Wang, W. (2023). Recognition of rock materials after high-temperature deterioration based on SEM images via deep learning. *J. Mater. Res. Technol.* 25, 273–284. doi:10.1016/j.jmrt.2023.05.271
- Huang, F., Cao, Z., Guo, J., Jiang, S. H., Li, S., and Guo, Z. (2020a). Comparisons of heuristic, general statistical, and machine learning models for landslide susceptibility prediction and mapping. *Catena* 191, 104580. doi:10.1016/j.catena.2020.104580
- Huang, F., Cao, Z., Jiang, S. H., Zhou, C., Huang, J., and Guo, Z. (2020b). Landslide susceptibility prediction based on a semi-supervised multiple-layer perceptron model. *Landslides* 17, 2919–2930. doi:10.1007/s10346-020-01473-9
- Huang, F., Chen, J., Liu, W., Huang, J., Hong, H., and Chen, W. (2022). Regional rainfall-induced landslide hazard warning based on landslide susceptibility mapping and a critical rainfall threshold. *Geomorphology* 408, 108236. doi:10.1016/j.geomorph.2022.108236
- Hur, M. W., and Park, T. W. (2022). Seismic performance of story-added type buildings remodeled with story seismic isolation systems. *Buildings* 3, 270. doi:10.3390/BUILDINGS12030270
- Jin, J. M., Tan, P., Zhou, F. L., Ma, Y. H., and Shen, C. Y. (2012). Shaking table test study on mid-story isolation structures. *Adv. Mater. Res.* 446, 378–381. Trans Tech Publications Ltd. doi:10.4028/scientific5/amr.446-449.378
- Li, W. F., Wang, S. G., and Miao, Q. S. (2014). Nonlinear simulation of reinforced masonry structure and adding-story isolation model. *China Civ. Eng. J.* 47 (S2), 35–40.
- Li, X., Zhang, X., Shen, W., Zeng, Q., Chen, P., Qin, Q., et al. (2023). Research on the mechanism and control technology of coal wall sloughing in the ultra-large mining height working face. *Int. J. Environ. Res. Public Health* 20 (1), 868. doi:10.3390/ijerph20010868
- Li, Z., Huang, G., Chen, X., and Zhou, X. (2022). Seismic response and parametric analysis of inter-story isolated tall buildings based on enhanced simplified dynamic model. *Int. J. Struct. Stab. Dyn.* 22, 03n04. doi:10.1142/S0219455422400089
- Li, Z., Huang, G., Chen, X., and Zhou, X. (2022). Seismic response and parametric analysis of inter-story isolated tall buildings based on the enhanced simplified dynamic model. *Int. J. Struct. Stab. Dyn.* 22 (03n04), 2240008. doi:10.1142/S0219455422400089
- Liang, Q., Jinyuan, W., and Li, L. (2023). Seismic control of story isolation system using tuned mass damper inerter. *J. Eng. Mech.* 149 (3). doi:10.1061/JENMDT.EMENG-6850
- Liao, W. I., Loh, C. H., and Wan, S. (2001). Earthquake responses of RC moment frames subjected to near-fault ground motions. *Struct. Des. Tall Build.* 10 (3), 219–229. doi:10.1002/tal.178
- Liu, D., Li, L., Zhang, Y., Chen, L., Wan, F., and Yang, F. (2022). Study on seismic response of a new staggered story isolated structure considering SSI effect. *J. Civ. Eng. Manag.* 28 (5), 397–407. doi:10.3846/jcem.2022.16825
- Liu, S., and Li, X. (2023). Experimental study on the effect of cold soaking with liquid nitrogen on the coal chemical and microstructural characteristics. *Environ. Sci. Pollut. Res.* 30 (13), 36080–36097. doi:10.1007/s11356-022-24821-9
- Liu, S., Sun, H., Zhang, D., Yang, K., Li, X., Wang, D., et al. (2023a). Experimental study of effect of liquid nitrogen cold soaking on coal pore structure and fractal characteristics. *Energy* 275, 127470. doi:10.1016/j.energy.2023.127470
- Liu, S., Sun, H., Zhang, D., Yang, K., Wang, D., Li, X., et al. (2023b). Nuclear magnetic resonance study on the influence of liquid nitrogen cold soaking on the pore structure of different coals. *Phys. Fluids* 35 (1), 012009. doi:10.1063/5.0135290
- Peng, T., and Dong, Y. (2023). Seismic responses of aqueducts using a new type of self-centering seismic isolation bearing. *Sustainability* 3, 2402. doi:10.3390/SU15032402
- Ryan, K. L., and Earl, C. L. (2010). Analysis and design of inter-story isolation systems with nonlinear devices. *J. Earthq. Eng.* 14 (7), 1044–1062. doi:10.1080/13632461003668020
- Song, L. U. O., Gong, F. Q., Li, L. L., and Peng, K. (2023). Linear energy storage and dissipation laws and damage evolution characteristics of rock under triaxial cyclic compression with different confining pressures. *Transactions of Nonferrous Metals Society of China* 33 (7), 2168–2182
- Toshiyuki, S., Shingo, T., and Yasuhiro, T. (2008). Response control design of Tokyo Shiodome Sumitomo mansion with seismic isolation interface at mid building. *Prog. Build. steel Struct.* (03), 36–41.
- Tasaka, M., Mori, N., Yamamoto, H., Murakami, K., and Sueoka, T. (2008). “Applying seismic isolation to buildings in Japan—Retrofitting and middle-story isolation”. In Structures Congress 2008: 18th Analysis and Computation Specialty Conference, 1–11.
- Wan, F., Cheng, L., Hong, L., Liu, D., Yao, S., and Lei, M. (2023). Seismic response of a mid-story-isolated structure considering soil-Structure interaction in sloping ground under three-dimensional earthquakes. *Front. Earth Sci.* 10. doi:10.3389/FEART.2022.1098711
- Zhang, J., Li, X., Qin, Q., Wang, Y., and Gao, X. (2023). Study on overlying strata movement patterns and mechanisms in super-large mining height stopes. *Bull. Eng. Geol. Environ.* 82 (4), 142. doi:10.1007/s10064-023-03185-5
- Zhang, L., Shen, W., Li, X., Wang, Y., Qin, Q., Lu, X., et al. (2022). Abutment pressure distribution law and support analysis of super large mining height face. *Int. J. Environ. Res. Public Health* 20 (1), 227. doi:10.3390/ijerph20010227
- Zhang, R., Phillips, B. M., Taniguchi, S., Ikenaga, M., and Ikago, K. (2017). Shake table real-time hybrid simulation techniques for the performance evaluation of buildings with inter-story isolation. *Struct. Control Health Monit.* 24 (10), e1971. doi:10.1002/stc.1971
- Zhang, S., Liu, F., Hu, Y., Li, S., and Zhu, L. (2021). Study on seismic response characteristics of the interlayer isolation structure. *J. Vibroengineering* 23 (8), 1765–1784. doi:10.21595/jve.2021.22003
- Zhou, Q., Singh, M. P., and Huang, X. Y. (2016). Model reduction and optimal parameters of mid-story isolation systems. *Eng. Struct.* 124, 36–48. doi:10.1016/j.engstruct.2016.06.011